Nonlinear Multi-Scale Model Order Reduction of Eddy-Current Problems

AUTHOR(S):

Eskandari, Hamed; Gyselinck, Johan; Matsuo, Tetsuji

Nonlinear Multi-Scale Model Order Reduction of Eddy-Current Problems

Hamed Eskandari[1], Johan Gyselinck[2], and Tetsuji Matsuo[1]
[1]Graduate School of Engineering, Kyoto University, Kyoto, 615-8510 Japan
[2] Universite Libre de Bruxelles (ULB), Department of Electrical Engineering, Brussels B-1050, Belgium

This paper presents a nonlinear multi-scale Model Order Reduction (MOR) method based on a piece-wise linearization technique. On the material scale, the eddy-current (EC) field in laminated cores is expressed through Legendre polynomials. The Cauer Ladder Network (CLN) method is applied to the homogenized nonlinear EC problem to generate the equivalent electric circuit. The accuracy and efficiency of the proposed method are verified by mean of a test case with saturated stacked core and Pulse Width Modulation (PWM) excitation.

***Index Terms*—Cauer Ladder Network, Nonlinear Eddy-Current, Laminated Core, Parametric Model Order Reduction, Multi-Scale.**

I. Introduction

OPTIMAL design of electromagnetic drive systems requires coupled analysis of equipment with their control units. The accuracy of the model is as essential as the intrinsic performance of the control strategy. Such models are expected to allow for the behavior of high-frequency eddy currents in the case of PWM excitation.

In most electromagnetic devices, stacked silicon steel sheets are used as iron cores. Accurate evaluation of fine-scale field fluctuation at the level of the sheets requires a fine division along the sheet thickness direction. The minimum grid should be at least in skin depth scale, i.e. as small as 0.05mm in typical power electronic applications. This can easily exceed the available computational resources. On the other hand, considering the magnetic saturation is inevitable since in practical applications electric machines ought to operate beyond the knee point of the magnetization curve to meet the power density requirements.

These issues have stimulated researches toward reduced-order models via the linear/nonlinear finite element (FE) method, generally known as MOR. Some of the MORs tackle the homogenization and expressing the behavior of electromagnetic equipment with microscopic structures, such as stacked steel sheets [1]–[3].

The other type of MORs aims for efficient electromagnetic field calculation over the whole machine on the machine scale. Proper orthogonal decomposition [4] and Krylov subspace method [5] are among the most popular machine scale MOR methods in recent literature. Some of the MOR approaches are capable of generating equivalent circuit models such as Padé via Lanczos (PVL) approximation to Krylov subspace [6] or the Cauer Ladder Network (CLN) method [7]. Several extensions were proposed to the CLN method, including nonlinear CLN [8], [9] and multi-scale MOR [10], [11]. The multi-scale MOR combines the homogenization method as a microscopic MOR and the CLN method as a machine scale MOR to construct an efficient and accurate reduced system including the laminated core [10].

To handle the saturable laminated core, a nonlinear version of multiscale MOR is required [12]. However, the nonlinearized homogenization method has always been a big challenge and is a fortiori so when applied to the multi-scale MOR. This paper develops the nonlinear multi-scale MOR based on a piece-wise linearization technique. The main contribution of this work is to consistently combine the nonlinear homogenization method with the CLN method to generate the equivalent circuit model for nonlinear laminated iron cores.

Manuscript received December 1, 2012; revised August 26, 2015. Corresponding author: H. Eskandari (email: hamed.eskandari.28x@st.kyoto-u.ac.jp).

II. Discrete Form of the EC Problem

The proposed method is easier to present if the fields are expressed in their discrete forms in the FE context although it is valid over continuous formulation too. The EC problem in a bounded domain $\Omega \in \mathbb{R}^3$ is subdivided into a set of finite elements. Then, to the edges and facets of the elements are associated basis vector functions $\boldsymbol{w}_i^1$ $(i = 1, \cdots, n_e)$ and $\boldsymbol{w}_j^2$ $(j = 1, \cdots, n_f)$, respectively, where n_e and n_f are the number of degrees of freedom associated to edges and facets, respectively. Finally, edge and facet quantities such as magnetic vector potential $\boldsymbol{A}$ and flux density $\boldsymbol{B}$ are expressed by column vectors $\boldsymbol{a} = [a_1, a_2, \cdots, a_{n_e}]^T$ and $\boldsymbol{b} = [b_1, b_2, \cdots, b_{n_f}]^T$, where a_i is the line integral of $\boldsymbol{A}$ over edge i, and b_j the surface integral of $\boldsymbol{B}$ on facet j [13].

The matrix formulation of the EC problem is given by

$$\begin{aligned} \boldsymbol{C}^T\boldsymbol{h} = \boldsymbol{C}^T\boldsymbol{\nu}\boldsymbol{C}\boldsymbol{a} = \boldsymbol{\sigma}\boldsymbol{e} + \boldsymbol{j}_0, \\ \boldsymbol{C}\boldsymbol{e} = -\partial_t\boldsymbol{b} = -\partial_t\boldsymbol{C}\boldsymbol{a}, \end{aligned} \tag{1}$$

where $\boldsymbol{C}$ is the edge-facet incident matrix, $\boldsymbol{h}$ and $\boldsymbol{j}_0$ are the discretized magnetic field intensity and external current density, and $\boldsymbol{\nu}$ and $\boldsymbol{\sigma}$ are the reluctivity and conductivity matrices given by

$$\boldsymbol{\nu} = \{\nu[i,j]\}, \quad \nu[i,j] = (\boldsymbol{w}_i^2, \frac{1}{\mu}\boldsymbol{w}_j^2)_\Omega, \tag{2}$$

$$\boldsymbol{\sigma} = \{\sigma[i,j]\}, \quad \sigma[i,j] = \left(\boldsymbol{w}_i^1, \sigma\boldsymbol{w}_j^1\right)_\Omega, \tag{3}$$

where σ and μ are the conductivity and permeability, and $(\cdot,\cdot)_\Omega$ denotes the volume integral of the scalar product of the two vector arguments.

III. Multi-Scale MOR

The multi-scale MOR in a nutshell is about employing MORs consecutively at different scales. This section briefly describes the implementation of the CLN method (as a macroscopic MOR) in a homogenized EC problem (as a microscopic MOR) in its general form.

A. Material Level MOR

Elaborate material level MORs are proposed to characterize the homogenized properties of stacked cores [1]–[3]. In [1], a homogenization method is presented in which the magnetic flux distribution in a steel sheet is characterized with Legendre polynomials $P_{2n}(-1 \le x \le 1, n = 0, 1, \cdots)$ as

$$\boldsymbol{B}(t,z) = \boldsymbol{b}_0(t)P_0\left(\frac{2z}{d}\right) + \boldsymbol{b}_2(t)P_2\left(\frac{2z}{d}\right) + \cdots \quad (4)$$

where d is the lamination thickness, z the coordinate in the stacking direction, and $\boldsymbol{b}_0, \boldsymbol{b}_2, \cdots$ the homogenized components of $\boldsymbol{B}$. Solving the 1-D EC problem inside the sheet links the surface magnetic field intensity, $\boldsymbol{H}_s(t)$, the average flux density $\boldsymbol{b}_0$, and the truncated homogenized components by

$$\begin{aligned}
\frac{1}{\mu}\boldsymbol{b}_0(t) =& \boldsymbol{H}_s(t) + \frac{\sigma d^2}{60}\frac{\mathrm{d}\boldsymbol{b}_2}{\mathrm{d}t} - \frac{\sigma d^2}{12}\frac{\mathrm{d}\boldsymbol{b}_0}{\mathrm{d}t},\\
\frac{1}{\mu}\boldsymbol{b}_{2n}(t) =& \frac{1}{4n+3}\frac{\sigma d^2}{4(4n+5)}\frac{\mathrm{d}\boldsymbol{b}_{2n+2}}{\mathrm{d}t}\\
&- \left(\frac{1}{4n+3} + \frac{1}{4n-1}\right)\frac{\sigma d^2}{4(4n+1)}\frac{\mathrm{d}\boldsymbol{b}_{2n}}{\mathrm{d}t}\\
&+ \frac{1}{4n-1}\frac{\sigma d^2}{4(4n-3)}\frac{\mathrm{d}\boldsymbol{b}_{2n-2}}{\mathrm{d}t}, \quad (1 \le n \le N) \quad (5)
\end{aligned}$$

where N is the number of homogenized components and $\boldsymbol{b}_{2n+2}$ is truncated.

This brings a new homogenized EC problem governed by

$$\underline{\boldsymbol{C}}^T\boldsymbol{\nu}'\underline{\boldsymbol{C}}\ \underline{\boldsymbol{a}} = -\left(\boldsymbol{\sigma}'_{nl} + \underline{\boldsymbol{C}}^T\boldsymbol{\sigma}'_l\underline{\boldsymbol{C}}\right)\partial_t\underline{\boldsymbol{a}} + \underline{\boldsymbol{j}}_0, \quad (6)$$

where matrices and vectors are represented blockwise as

$$\begin{aligned}
\boldsymbol{\nu}' &= \mathrm{blockdiag}\left\{\boldsymbol{\nu}_H, \frac{\boldsymbol{\nu}_l}{5}, \cdots, \frac{\boldsymbol{\nu}_l}{4N+1}\right\},\\
\boldsymbol{\sigma}'_{nl} &= \mathrm{blockdiag}\left\{\boldsymbol{\sigma}_{nl}, 0, \cdots, 0\right\},\\
\boldsymbol{\sigma}'_l &= \{\boldsymbol{\sigma}^*_l[i,j]\}, \quad \boldsymbol{\sigma}^*_l[0,0] = \frac{\boldsymbol{\sigma}_l d^2}{12}\\
\boldsymbol{\sigma}^*_l[n,n] &= \left(\frac{1}{4n+3} + \frac{1}{4n-1}\right)\frac{\boldsymbol{\sigma}_l d^2}{4(4n+1)^2}, \ (1 \le n)\\
\boldsymbol{\sigma}^*_l[n+1,n] &= \boldsymbol{\sigma}^*_l[n,n+1]\\
&= \frac{-\boldsymbol{\sigma}_l d^2}{4(4n+1)(4n+3)(4n+5)},\\
\underline{\boldsymbol{C}} &= \mathrm{blockdiag}\left\{\boldsymbol{C}_H, \boldsymbol{C}_l, \cdots, \boldsymbol{C}_l\right\},\\
\underline{\boldsymbol{a}} &= \left[\boldsymbol{a}_0^T, \boldsymbol{a}_{2,l}^T, \cdots, \boldsymbol{a}_{2N,l}^T\right]^T, \quad \underline{\boldsymbol{j}}_0 = \left[\boldsymbol{j}_0^T, 0, \cdots, 0\right]^T, \quad (7)
\end{aligned}$$

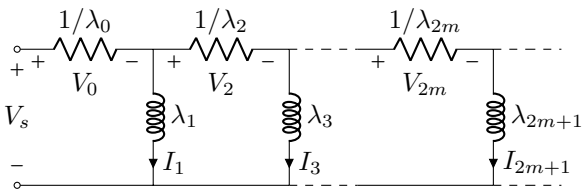

Fig. 1. Cauer ladder network.

where the subscripts l, nl and H refers to the laminated, non-laminated and the whole domain, respectively. For the sake of brevity homogenized coefficient matrices $\boldsymbol{K}'$ and $\boldsymbol{\sigma}'$ are defined as $\boldsymbol{K}' = \underline{\boldsymbol{C}}^T\boldsymbol{\nu}'\underline{\boldsymbol{C}}$ and $\boldsymbol{\sigma}' = \boldsymbol{\sigma}'_{nl} + \underline{\boldsymbol{C}}^T\boldsymbol{\sigma}'_l\underline{\boldsymbol{C}}$. Using the averaging process in [1], the permeability and conductivity in Ω_l are amended to $\alpha\mu$ and $\alpha\sigma$, with α the fill factor of the stacked core ($0 < \alpha \le 1$). The homogenized reluctivity and conductivity matrices are given by

$$\begin{aligned}
\boldsymbol{\nu}_l &= \{\nu_l[i,j]\}, & \nu_l[i,j] &= ((\alpha\mu)^{-1}\boldsymbol{w}_i^2, \boldsymbol{w}_j^2)_{\Omega_l},\\
\boldsymbol{\nu}_H &= \{\nu_H[i,j]\}, & \nu_H[i,j] &= \nu_l[i,j] + (\mu_0^{-1}\boldsymbol{w}_i^2, \boldsymbol{w}_j^2)_{\Omega_{nl}},\\
\boldsymbol{\sigma}_l &= \{\sigma_l[i,j]\}, & \sigma_l[i,j] &= (\alpha\sigma\boldsymbol{w}_i^2, \boldsymbol{w}_j^2)_{\Omega_l},\\
\boldsymbol{\sigma}_{nl} &= \{\sigma_{nl}[i,j]\}, & \sigma_{nl}[i,j] &= (\sigma\boldsymbol{w}_i^1, \boldsymbol{w}_j^1)_{\Omega_{nl}}. \quad (8)
\end{aligned}$$

where Ω_{nl} is the non-laminated region with the vacuum permeability μ_0.

B. Machine Level MOR

The order of (6) can be further reduced at a machine level by means of the CLN method [7]. To do so, $\underline{\boldsymbol{a}}$ and $\underline{\boldsymbol{e}} = -\partial_t\underline{\boldsymbol{a}}$ are expressed by orthogonal modes and associated transient scalar coefficients:

$$\begin{aligned}
\underline{\boldsymbol{a}}(t) &= \sum_m I_{2m+1}(t)\ \underline{\boldsymbol{a}}_{2m+1},\\
\underline{\boldsymbol{e}}(t) &= \sum_m V_{2m}(t)\ \underline{\boldsymbol{e}}_{2m}. \quad (9)
\end{aligned}$$

The orthogonal basis vectors are generated recursively as

$$\begin{aligned}
\lambda_{2m} &= \underline{\boldsymbol{e}}_{2m}^T\boldsymbol{\sigma}'\underline{\boldsymbol{e}}_{2m},\\
\boldsymbol{K}'(\underline{\boldsymbol{a}}_{2m+1} - \underline{\boldsymbol{a}}_{2m-1}) &= \frac{1}{\lambda_{2m}}\boldsymbol{\sigma}'\underline{\boldsymbol{e}}_{2m},\\
\lambda_{2m+1} &= \underline{\boldsymbol{a}}_{2m+1}^T\boldsymbol{K}'\underline{\boldsymbol{a}}_{2m+1},\\
\underline{\boldsymbol{e}}_{2m+2} - \underline{\boldsymbol{e}}_{2m} &= \frac{-1}{\lambda_{2m+1}}\underline{\boldsymbol{a}}_{2m+1}, \quad (10)
\end{aligned}$$

starting with $\underline{\boldsymbol{a}}_{-1} = 0$ and $\underline{\boldsymbol{e}}_0$ corresponding to the electric field generated by a unit dc excitation voltage applied to the excitation coil.

Transient coefficients are also obtained from the circuit equations as

$$\begin{aligned}
V_0 &= V_s - \lambda_1\partial_t I_1,\\
V_{2m+2} &= \lambda_{2m+1}\partial_t I_{2m+1} - \lambda_{2m+3}\partial_t I_{2m+3},\\
I_{2m+1} &= \lambda_{2m}V_{2m} - \lambda_{2m+2}V_{2m+2}, \ (m = 0, 1, \cdots) \quad (11)
\end{aligned}$$

where V_s is the input source voltage.

With constant homogeneous magnetic permeability, (11) is equivalent to the Cauer ladder network where $R_{2m} = 1/\lambda_{2m}$ and $L_{2m+1} = \lambda_{2m+1}$ as depicted in Fig. 1.

IV. Nonlinear Multi-Scale MOR

The multi-scale MOR in section III was first presented in [10], where the homogenization and the CLN were both limited to the linear magnetic materials. In many practical electromagnetic apparatus, the core is operated under saturation. This section aims to present a nonlinear analysis, compatible with both of the MORs.

A. Nonlinear Homogenization

There are several approaches proposed to solve (6) on a nonlinear medium. Some of those methods have intrinsic consistency with the CLN. In [2], (6) is solved by applying the Newton-Raphson scheme to the nonlinear algebraic equations obtained after time discretization. Its accuracy has been validated over a wide range of frequency; the first drawback is the computational cost due to the numerical integration along the lamination thickness to calculate the Jacobian matrix. The other disadvantage is the incompatibility with the CLN approach.

In [3], the magnetic field intensity in material scale for an isotropic, non-hysteric material characterized with $|\boldsymbol{H}| = H_{dc}(|\boldsymbol{B}|)$, is approximated by

$$\begin{aligned}\boldsymbol{H}(t,z) &= \boldsymbol{H}_{dc}(\boldsymbol{b}_0(t) + \boldsymbol{b}_2(t)P_2 + \boldsymbol{b}_4 P_4 + \cdots) \\ &\approx \boldsymbol{H}_{dc}(\boldsymbol{b}_0(t)) + \frac{\boldsymbol{b}_2(t)P_2 + \boldsymbol{b}_4(t)P_4 + \cdots}{\mu^d(\boldsymbol{b}_0(t))} \end{aligned} \tag{12}$$

where $\mu^d = \mathrm{d}|\boldsymbol{B}|/\mathrm{d}|\boldsymbol{H}|$ is the differential permeability. In contrast to [2], on (12) the permeability is considered frozen along the lamination thickness, which makes it less accurate, but computationally cheap and interoperable with the CLN.

B. Nonlinear CLN

The linearization in the machine scale in the CLN context is investigated in [8], [9]. Sato and Igarashi [8], considered the magnetic saturation by imposing the nonlinearity on the first inductor L_1, only. In [9], the nonlinearity was extended to all the circuit elements similar to (12) except that all of the magnetic modes are interpolated with μ or μ^d only.

The close analogy in the microscopic linearization [3] and the macroscopic one [9] brings up the nonlinear multi-scale MOR procedure summarized in algorithm 1. A table of parametric CLN elements are computed with respect to the coil current I_1 in line 4. On line 5, two definitions to nonlinear permeability are adopted by μ and μ^d and are presumed for construction of $\boldsymbol{K}'^{(d)}$. The superscript (d) represents either apparent of differential definitions. By neglecting the transition of magnetic modes at two consecutive time-steps, the network equations become identical to that of the first-order approximation method (FO-CLN) [9].

According to the FO-CLN, the circuit equations (11) are approximated in two distinct ways depending on the adoption of μ or μ^d.

Algorithm 1 Nonlinear Multi-Scale MOR Procedure

1: $\underline{\boldsymbol{a}}_{-1} = 0, \boldsymbol{e}_0 : given, \underline{\boldsymbol{e}}_0 = [\boldsymbol{e}_0^T, 0, \cdots]^T$
2: $\lambda_0 = \underline{\boldsymbol{e}}_0^T \boldsymbol{\sigma}' \underline{\boldsymbol{e}}_0$
3: **for** all feasible I_1 **do**
4: $\quad solve : \nabla \times [\boldsymbol{H}_{dc}(\boldsymbol{B}_{dc})] = I_1 \lambda_0^{-1} \boldsymbol{\sigma}_{nl} \boldsymbol{e}_0$
5: $\quad \mu_{I_1} = |\boldsymbol{B}_{dc}|/|\boldsymbol{H}_{dc}|$ *or* $\mu^d_{I_1} = \mathrm{d}|\boldsymbol{B}_{dc}|/\mathrm{d}|\boldsymbol{H}_{dc}|$
6: $\quad$ **for** $n = 0$ **to** $n = \#stages$ **do**
7: $\quad\quad solve : \boldsymbol{K}'^{(d)} \tilde{\underline{\boldsymbol{a}}}_{2n+1} = \boldsymbol{\sigma}' \underline{\boldsymbol{e}}_{2n} / \lambda^{(d)}_{2n}(I_1)$
8: $\quad\quad \underline{\boldsymbol{a}}_{2n+1} = \tilde{\underline{\boldsymbol{a}}}_{2n+1} + \underline{\boldsymbol{a}}_{2n-1}$
9: $\quad\quad \lambda^{(d)}_{2n+1}(I_1) = \underline{\boldsymbol{a}}^T_{2n+1} \boldsymbol{K}'^{(d)} \underline{\boldsymbol{a}}_{2n+1}$
10: $\quad\quad \underline{\boldsymbol{e}}_{2n+2} = \underline{\boldsymbol{e}}_{2n} - \underline{\boldsymbol{a}}_{2n+1} / \lambda^{(d)}_{2n+1}(I_1)$
11: $\quad\quad \lambda^{(d)}_{2n+2}(I_1) = \underline{\boldsymbol{e}}^T_{2n+2} \boldsymbol{\sigma}' \underline{\boldsymbol{e}}_{2n+2}$
12: $\quad$ **end for**
13: **end for**

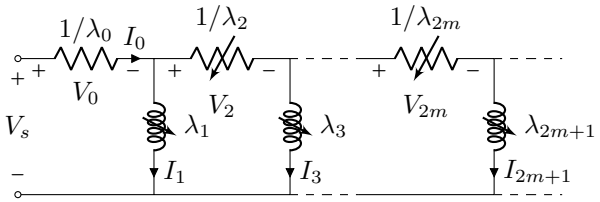

Fig. 2. Parametric Cauer ladder network.

1) Apparent permeability

In the case of apparent permeability the voltages in (11) are approximated by

$$\begin{aligned} V_0 &= V_s - \frac{\mathrm{d}(\lambda_1(|I_0|)I_1)}{\mathrm{d}t}, \\ V_{2m+2} &= \frac{\mathrm{d}(\lambda_{2m+1}(|I_0|)I_{2m+1})}{\mathrm{d}t} \\ &\quad - \frac{\mathrm{d}(\lambda_{2m+3}(|I_0|)I_{2m+3})}{\mathrm{d}t}, \ (m = 0, 1, \cdots) \end{aligned} \tag{13}$$

where

$$\lambda_m(|I_0|) = \lambda_m(I_1)\big|_{I_1 = |I_0|}. \tag{14}$$

2) Differential permeability

If algorithm 1 is performed by μ^d then

$$\begin{aligned} V_0 &= V_s - \lambda^d_1(|I_1|)\frac{\mathrm{d}I_1}{\mathrm{d}t}, \\ V_{2m+2} &= \lambda^d_{2m+1}(|I_{2m+1}|)\frac{\mathrm{d}I_{2m+1}}{\mathrm{d}t} \\ &\quad - \lambda^d_{2m+3}(|I_{2m+3}|)\frac{\mathrm{d}I_{2m+3}}{\mathrm{d}t}. \ (m = 0, 1, \ \ldots) \end{aligned} \tag{15}$$

where

$$\lambda_m(|I_m|) = \lambda_m(I_1)\big|_{I_1 = |I_m|}. \tag{16}$$

V. Numerical Example

To validate the proposed method, we solve an EC problem in a laminated inductor with 10 sheets of 20×0.5mm extended to infinity along the z direction, enclosed with a single turn massive coil with thickness and fill-factor of 0.2mm and 90%, respectively. By exploiting the symmetry of the problem only one quarter of the inductor is modeled and illustrated in

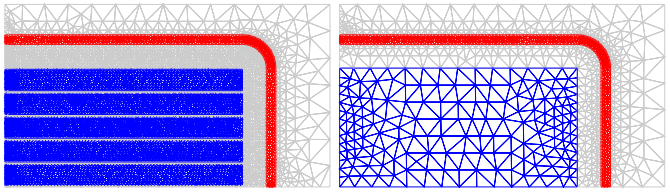

Fig. 3. FE meshes used in (a) RM and (b) homogenized model.

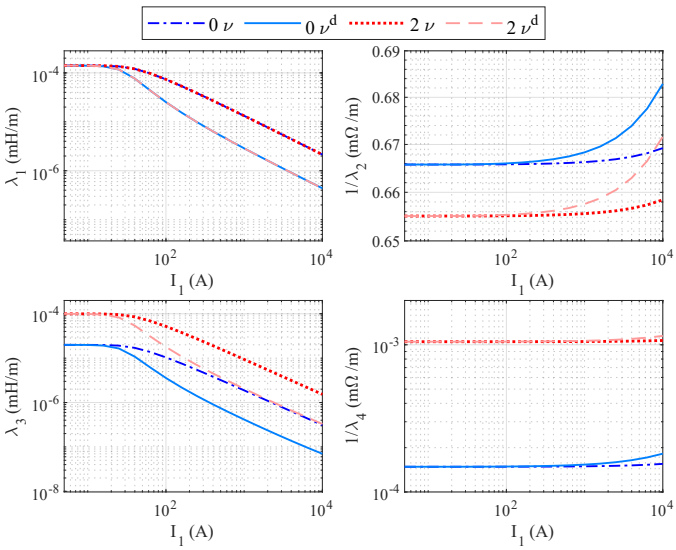

Fig. 4. Resistances and inductances of the nonlinear CLN circuit given by μ and μ^d.

Fig. 3,where Figs 3(a) and (b) show the FE meshes used in the reference model (RM) and the homogenized model. The conductivity of the coil and sheets are set to 40MS/m and 1MS/m, respectively. The nonlinear magnetic characteristic of the lamination is expressed by

$$H = 10000\nu_0 \left[5\left(\frac{B}{B_0}\right)^4 + 1\right] B, \tag{17}$$

with ν_0 the vacuum reluctivity and $B_0 = 1$ T.

A. Equivalent Circuits

The proposed method is implemented on (6) with $N = 0$ and $N = 1$ as 0^{th} and 2^{nd} order homogenization, resulting in four equivalent circuits. Fig. 4 demonstrates the variation of CLN elements with respect to the coil current. As shown in Fig. 2, the first resistor λ_0 which corresponds to the coil conductance is invariant to the saturation level and is equal to 0.95MS/m.

B. Global Quantities

The coil is excited with PWM voltage with fundamental and carrier frequencies of 50Hz and 3kHz, respectively. Fig. 5 illustrates the currents obtained from solving (1) via FE (RM) and the four parametric CLNs; they are high enough for saturating the core. The results are also magnified at maximum

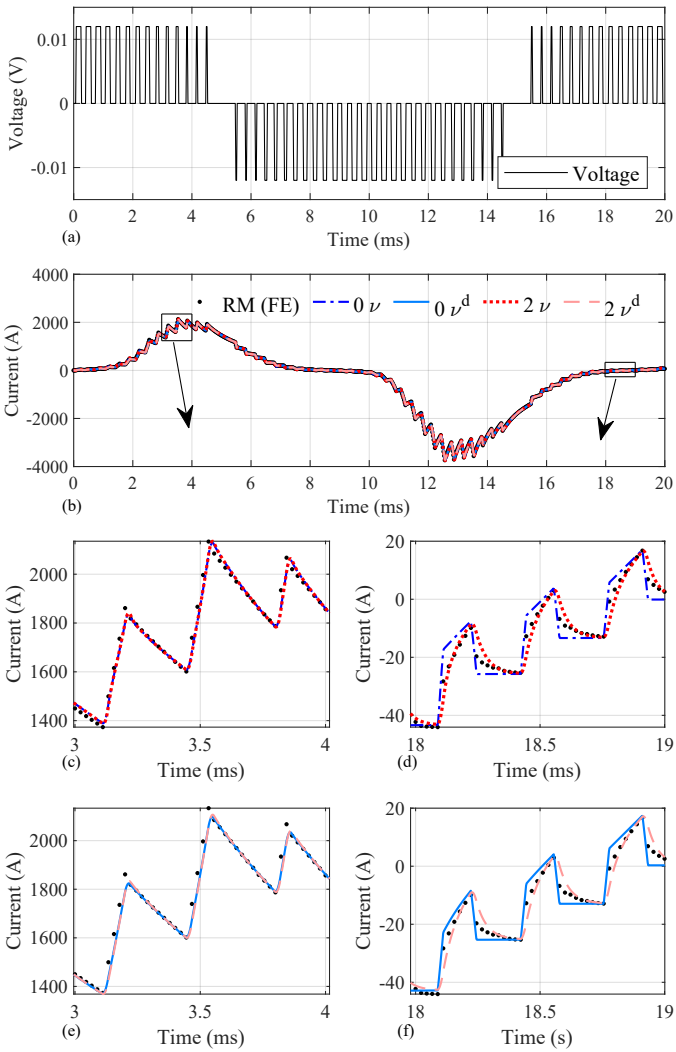

Fig. 5. Transient analysis results, (a) input voltage, (b) current waveforms, (c) enlarged view of the first box showing 0^{th} and 2^{nd} order hom. via apparent permeability, (d) enlarged view of the second box showing 0^{th} and 2^{nd} order hom. via apparent permeability (e) enlarged view of the first box showing 0^{th} and 2^{nd} order hom. via differential permeability, (f) enlarged view of the second box showing 0^{th} and 2^{nd} order hom. via differential permeability

saturation and zero-crossing time intervals. When the core is highly saturated, the permeability decreases enough to increase the skin depth and extinguish the effect of EC. It justifies the conformity of 0^{th} and 2^{nd} order results in Fig. 5(c) and (e). Around the zero-crossing points, Fig. 5(d) and (f), the networks obtained from 2^{nd} order homogenizations clearly outperform the 0^{th} order counterparts.

C. Local Quantities

It is feasible to reconstruct the field values $\boldsymbol{B}(t, z)$ by (9). However on nonlinear case, the field reconstruction depends on the selection of μ or μ^d in algorithm 1. First of all, It is required to store the distribution of reluctivities $\boldsymbol{\nu}^{(d)}(I_1)$ and the field values $\underline{\boldsymbol{a}}_{2m+1}(I_1)$. Then, the homogenized components of the magnetic modes should be decomposed into

$$\underline{\boldsymbol{a}}_{2m+1} = \left[\boldsymbol{a}^T_{0,2m+1}, \cdots, \boldsymbol{a}^T_{2N,2m+1}\right]^T, \tag{18}$$

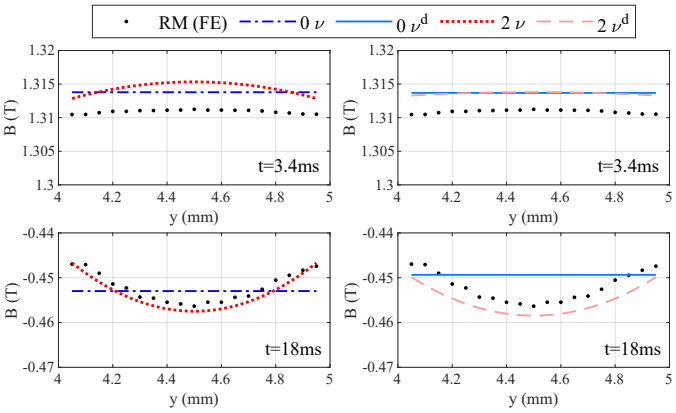

Fig. 6. The reconstructed field at the center-line of the lamination on the top.

where, e.g., $\boldsymbol{a}^T_{0,2m+1}$ is the first component of the $2m+1^{th}$ mode. The rest of the operation depends on the choice of μ or μ^d.

1) Apparent permeability

If the nonlinear multi-scale MOR is derived with μ, then

$$\begin{aligned}\boldsymbol{B}(t,z) = P_0(\frac{2z}{d})\sum_m \frac{I_{2m+1}(t)}{\alpha}\boldsymbol{C}_H\boldsymbol{a}_{0,2m+1}(|I_0(t)|)\\ + P_2(\frac{2z}{d})\sum_m \frac{I_{2m+1}(t)}{\alpha}\boldsymbol{C}_l\boldsymbol{a}_{2,2m+1}(|I_0(t)|)\\ + \cdots .\end{aligned} \tag{19}$$

2) Differential permeability

In the case of differential permeability, the local field inside the laminations is obtained by

$$\begin{aligned}\boldsymbol{B}(t,z) = P_0(\frac{2z}{d})\sum_m \frac{I_{2m+1}(t)}{\alpha}\boldsymbol{\nu}_l^{-1}\boldsymbol{\nu}_l^d\boldsymbol{C}_H\boldsymbol{a}_{0,2m+1}(|I_{2m+1}|)\\ + P_2(\frac{2z}{d})\sum_m \frac{I_{2m+1}(t)}{\alpha}\boldsymbol{C}_l\boldsymbol{a}_{2,2m+1}(|I_{2m+1}|)\\ + \cdots .\end{aligned} \tag{20}$$

The reconstructed magnetic flux density on the center-line , $x = 0$, at $t = 3.4$ms and $t = 18$ms are shown in Fig. 6. It is clear that in sense of nonlinearity, all the cases provide high accuracy (i.e., at $t = 3.4$ms the average discrepancy with RM is less than 0.05T). Additionally, the parametric CLN obtained with the 2^{nd} order homogenization using μ^d, achieves slightly better accuracy. This is consistent with (12) where the operating point is approximated by μ and the small perturbations are modeled with μ^d.

D. Computational Time

The computational cost in time-domain is determined by the number of time-steps, which is 901 in the case of the results in Fig. 5. The time required to solve the RM with 5344 triangular elements and 2751 vertices is 2 hours and 20 minutes, using a computer with clock frequency of 2.9 GHz and 16.0 GB of RAM.

On the nonlinear-multi-scale MOR side, the computation of parametric elements dominates the total computational time, while the circuit equations require less resources. To obtain the parameters depicted in Fig. 4 with 20 points on I_1, it takes 65s and 78s for the 0^{th} and 2^{nd} order homogenizations, respectively. Solving the circuit equations (13) and (15) takes only 2s each. It means that the proposed multi-scale MOR yields a speed-up factor of at least 105 per cycle with negligible loss of accuracy.

VI. Conclusion

A coupled linearization technique was proposed to extend the multi-scale MOR to handle mediums with nonlinear magnetic properties. The developed procedures of generating parametric equivalent circuits, solving the state equations and field reconstructions were explained in detail. Finally, the proposed approach was verified via numerical examples. It has been shown that the proposed method has acceptable performance both in terms of accuracy and efficiency.

Acknowledgment

This work was supported in part by the Japan Society for the Promotion of Science under Grant-in-Aid for Scientific Research (C) 20K04443. The work of Hamed Eskandari was supported by the Yoshida Scholarship Foundation.

References

[1] J. Gyselinck, P. Dular, L. Krahenbuhl, and R. V. Sabariego, "Finite-element homogenization of laminated iron cores with inclusion of net circulating currents due to imperfect insulation," IEEE Trans. on Magn., vol. 52, no. 3, Art. no. 7209104, March 2016.
[2] J. Gyselinck, R. V. Sabariego and P. Dular, "A nonlinear time-domain homogenization technique for laminated iron cores in three-dimensional finite-element models," in IEEE Trans. on Magn., vol. 42, no. 4, pp. 763-766, April 2006.
[3] Y. Shindo, et. al., "Cauer circuit representation of the homogenized eddy-current field based on the legendre expansion for a magnetic sheet," IEEE Trans. on Magn., vol. 52, no. 3, Art no. 6300504, March 2016.
[4] T. Shimotani, Y. Sato, and H. Igarashi, "Equivalent-circuit generation from finite-element solution using proper orthogonal decomposition," IEEE Trans. Magn., vol. 52, no. 3, Art. no. 7206804, March 2016.
[5] R. W. Freund, "Krylov-subspace methods for reduced-order modeling in circuit simulation," J. Comput. Appl. Math., vol. 123, no. 1, pp. 395–421, 2000.
[6] Y. Sato and H. Igarashi, "Generation of equivalent circuit from finite element model using model order reduction," IEEE Trans. Magn., vol. 52, no. 3, Art. no. 1100304, March 2016.
[7] A. Kameari, et. al., "Cauer ladder network representation of eddy-current fields for model order reduction using finite-element method," IEEE Trans. on Magn., vol. 54, no. 3, Art. No. 7201804, March 2018.
[8] Y. Sato, T. Shimotani and H. Igarashi, "Synthesis of Cauer-Equivalent Circuit Based on Model Order Reduction Considering Nonlinear Magnetic Property," in IEEE Trans. on Magn., vol. 53, no. 6, Art no. 1100204, June 2017.
[9] H. Eskandari and T. Matsuo, "Comparison study of first-order approximations of nonlinear eddy-current field using Cauer ladder network method," in IEEE Trans. on Magn., doi: 10.1109/TMAG.2021.3060503.
[10] H. Eskandari, J. Gyselinck and T. Matsuo, "Eddy-current field analysis in laminated iron cores using multi-scale model order reduction," in IEEE Trans. on Magn., doi: 10.1109/TMAG.2021.3064410.
[11] S. Hiruma and H. Igarashi, "Synthesis of equivalent circuit from homogenized FE equation using model order reduction," IEEJ Trans. on Power and Energy, vol. 140, no. 2, pp. 134–139, 2020.
[12] K. Hollaus, J. Schöberl and M. Schöbinger, "MSFEM and MOR to minimize the computational costs of nonlinear eddy-current problems in laminated iron cores," in IEEE Trans. on Magn., vol. 56, no. 2, Art no. 7508104, Feb. 2020.
[13] A. Bossavit, Computational Electromagnetism, San Diego, CA, USA:Academic Press, 1998.